Fluorescent Tracing of Dialdehyde Sodium Alginate Tanning Agent in Leather Matrix

by
Min Zhu,[1] Yudan Yi,[1] Jia Fu,[1] Yunhang Zeng[1] and Ya-nan Wang[1,2,*]
[1]*National Engineering Laboratory for Clean Technology of Leather Manufacture,*
Sichuan University, Chengdu 610065, China
[2]*Key Laboratory of Leather Chemistry and Engineering of Ministry of Education,*
Sichuan University, Chengdu 610065, China

Abstract

Dialdehyde polysaccharides possess a sustainable nature and good tanning performance. However, the lack of specific detectable groups in their molecular structure results in the difficulty in the determination of the location of dialdehyde polysaccharides in leather fiber networks. In this study, dialdehyde sodium alginate (DSA) tanning agent was fluorescent labeled by 5-(4,6-dichlorotriazinyl) aminofluorescein (DTAF). The purified DTAF–DSA showed high and stable fluorescent intensity at emission wavelength of 515.2 nm when the pH was over 6.0, and the temperature was in the range of 20°C to 50°C. DTAF–DSA was used in tanning and tracked using fluorescence microscopy. Its penetration in the fiber network could be clearly visualized, and its distribution in leather differed with the molecular weight of DSA. As a result, this fluorescence tracing technique could display the mass transfer behavior of dialdehyde polysaccharide tanning agents in leather matrix, which will provide underlying data for tanning mechanism exploration.

Introduction

Tanning is the most essential process of leather-making to convert raw hide/skin into durable leather. Currently, the development of chrome-free tanning technologies to replace chrome tannage is in full swing[1-3] because of the potential environmental risk of hexavalent chromium.[4-6] In particular, a trend toward biomass-based chrome-free tanning system is emerging in recent years to support a more sustainable leather industry.[7-9] Polysaccharides and their derivatives, such as cellulose[10-12] starch[13-16] and alginate,[17-19] have been modified to produce biomass-based tanning agents. Among them, dialdehyde polysaccharides produced by periodate oxidation is regarded as a promising tanning agent due to its high reactivity and adjustable molecular size.[19-20] Degradation of polysaccharides via glycosidic bond breaking co-occurs with aldehyde group formation in periodate oxidation. However, the reported dialdehyde polysaccharide tanning agents exhibited molecular weights of in the thousands,[11,16,18] much higher than traditional tanning agents. This raised questions whether the dialdehyde polysaccharide tanning agent can penetrate the hierarchical hide/skin matrix and carry out tanning effectively. Unlike mineral tanning agents, the organic dialdehyde polysaccharide cannot be distinguished with collagen matrix by using EDS analysis.[21] Therefore, it is necessary to establish a method to monitor the penetration (mass transfer behavior) and distribution of dialdehyde polysaccharide tanning agent in leather, which in turn explores the effect of mass transfer on the tanning performance.

Fluorescent tracing technique can visually trace and display the distribution of leather chemicals in leather matrix. It has been applied in the location of enzymes,[22-24] acrylic resin retanning agents,[25-27] amino resin retanning agents[28,29] and fatliquors.[30-32] The brief procedure for this technique is described below. Fluorescein was used to label these chemicals via covalent binding at first. Then the fluorescent labeled chemical was introduced into skin/leather under the conventional conditions. Fluorescence microscopic techniques were used for the observation of skin/leather sections to achieve the location of the chemical within collagen fibers. Our previous work reported that aldehyde tanning agents could be visualized through the autofluorescence of Schiff base formed by aldehyde and amino groups of collagen. However, this approach was not sensitive enough to detect dialdehyde polysaccharides.[33] Fluorescent labeling may be more suitable for this type of tanning agent.

In this study, dialdehyde sodium alginate (DSA) was chosen as the model object of dialdehyde polysaccharide tanning agent due to its satisfactory tanning effects.[18,34] Considering that hydroxyl groups are the most common functional groups of polysaccharides, fluorescent labeling with the hydroxyl of DSA was performed in order to establish a universal method. Then the penetration and distribution of the fluorescent labeled DSAs with different molecular weights in the tanned leather was visualized using fluorescence microscopy to verify if this is an effective approach to characterize the mass transfer behavior of dialdehyde polysaccharide tanning agent.

*Corresponding author email: wangyanan@scu.edu.cn
Manuscript received March 5, 2023, accepted for publication April 8, 2023.

Experimental

Materials

Sodium alginate (SA), sodium periodate, ethanediol and ethanol were of analytical grade and purchased from Chengdu Kelong Chemical Co., Ltd (Chengdu, China). 5-(4,6-dichlorotriazinyl) aminofluorescein (DTAF) was purchased from Aladdin Biochemical Technology Co., Ltd (Shanghai, China). Sephadex G-25 was purchased from Sigma-Aldrich Co. LLC. All the chemicals used for the analyses were of analytical grade, and the chemicals used for leather processing were of commercial grade.

Preparation of DSA

DSA was prepared according to Ding's method.[18] Sodium periodate (17.28 g) was dissolved in 500 mL ultrapure water, and then 20.0 g SA was added during stirring. After stirring for 24 h in the dark, the reaction was terminated by 4.5 mL ethanediol for 0.5 h. The product solution was fractionated by ethanol precipitation as follows. Firstly, 55.56 mL ethanol was added to obtain 10% ethanol-water solution (v/v). After standing at 4°C for 72 h, the solution was filtered by vacuum filtration. Then, the filtrate was precipitated using 20% ethanol-water solution (v/v) by adding extra 69.45 mL ethanol at 4°C for 72 h. The precipitate was separated and purified by dialysis with ultrapure water as the dialysis medium (dialysis bag MWCO 300 Da), and the retentate was lyophilized into DSA with high molecular weight (H–DSA). The filtrate was precipitated using 35% ethanol-water solution (v/v) by adding extra 144.23 mL ethanol at 4°C for 72 h. DSA with moderate molecular weight (M–DSA) was obtained by separation and purification in the same way as above. In addition, 500 mL ethanol was added into the initial product solution at 4°C for 72 h. The precipitate was separated and purified by dialysis as well. The retentate was lyophilized into DSA with low molecular weight (L–DSA).

Fourier Transform Infrared (FT-IR) spectroscopy analysis

SA or DSA was mixed with potassium bromide powder and pressed into a tablet. Then the FT-IR spectra of SA and DSA were determined using a FT-IR spectrometer (Nicolet Is50, Thermo Fisher, USA). The wavenumber ranged from 500 to 4000 cm^{-1}. The resolution was 4 cm^{-1}, and the cumulative number of scans was 32.

Determination of aldehyde group content of DSA

The aldehyde group content of DSA was determined by hydroxylamine hydrochloride titration method.[35] In brief, freeze–dried DSA (0.1000 g) was dissolved in 25 mL ultrapure water. The pH value of the DSA solution was adjusted to 5.0 with HCl/NaOH solution. The pH of 20 mL hydroxylamine hydrochloride solution (0.25 mol/L) was adjusted to 5.0 with NaOH solution. The above two solutions were mixed evenly and reacted at 40°C for 4 h in a water bath shaker. Then, the pH of the mixture was titrated to 5.0 with 0.1 mol/L NaOH solution, and the volume of titrant was recorded to calculate the aldehyde group content of DSA.

Preparation of DTAF labeled DSA (DTAF–DSA)

DSAs with different molecular weights were labeled according to the method of Abitbol T et al. with some modifications.[36] Dichlorotriazine, the reactive group of DTAF, can covalently bind with hydroxyl of DSA. DSA (0.5 g) was reacted with 7.5 mg DTAF in 12.5 mL borax-NaOH buffer (pH 9.5) in the dark with stirring for 24 h. The product was concentrated with PEG-20000 to a final volume of 4 mL, filtered through 0.45 μm filter units, and then loaded onto a Sephadex G-25 gel-filtration column (1.6 cm × 50 cm) to remove unreacted DTAF. Borax/boric acid buffer (pH 9.0) was used as the mobile phase with a flow rate of 0.06 mL/min. The eluate fractions (3 mL/tube) were collected automatically, and the absorbance of each fraction was measured at 490 nm (the absorbance maximum of DTAF) using an UV–Vis spectrophotometer (UV–1899PC, Mapada, China). The DTFA–DSA fractions without DTAF were collected. Borax/boric acid were removed from the collected fractions via dialysis in ultrapure water (dialysis bag MWCO 300 Da) until the pH of dialysate reached 7.0. The retentate was lyophilized into DTAF–DSA.

Analysis of fluorescence emission spectra

Fluorescence emission spectra of DTAF (20 mg/L), DSA (100 mg/L), DTAF–H–DSA (100 mg/L), DTAF–M–DSA (100 mg/L) and DTAF–L–DSA (100 mg/L) were measured by fluorescence spectrophotometer (F–7100, Hitachi, Japan) with 492 nm excitation wavelength of (the excitation maximum of DTAF). Fluorescence emission was recorded from 500 to 620 nm.

Thermal and pH stability of DTAF–DSA

The temperature of DTAF–L–DSA solutions (100 mg/L) were held at 20°C, 25°C, 30°C, 35°C, 40°C, 45°C and 50°C, respectively, for 20 min. Then the fluorescence emission spectra of the solutions were determined with 492 nm excitation wavelength to evaluate the thermal stability of DTAF–DSA.

The pH values of DTAF–L–DSA solutions (100mg/L) were adjusted to 3.00, 4.00, 5.12, 6.17, 6.96, 8.05 and 8.96 with HCl/NaOH solution and held at room temperature for 1 h. Fluorescence emission spectra of these solutions were determined with an excitation wavelength of 492 nm to evaluate the pH stability of DTAF–DSA.

Determination of molecular weight

The size exclusion chromatography (SEC, 1260 Infinity II, Agilent, USA) was used to measure the weight average molecular mass (M_w) and polydispersity (PDI) of DSA and DTAF–DSA. The sample solution (5 mg/mL) was filtered through 0.45 μm filter units and then analyzed under the following conditions. The injection volume was 50 μL. A TSK-gel GMPWXL column (7.8 mm × 300 mm, Tosoh, Japan) was equipped. $NaNO_3$ solution (0.1 mol/L) was used as the mobile phase at a flow rate of 0.6 mL/min.[37] The column temperature was maintained at 30°C. Pullulan standards from 180 Da to 600 kDa (Agilent, UK) were used for calibration.[38] The results were processed with OmniSEC 4.7 software.

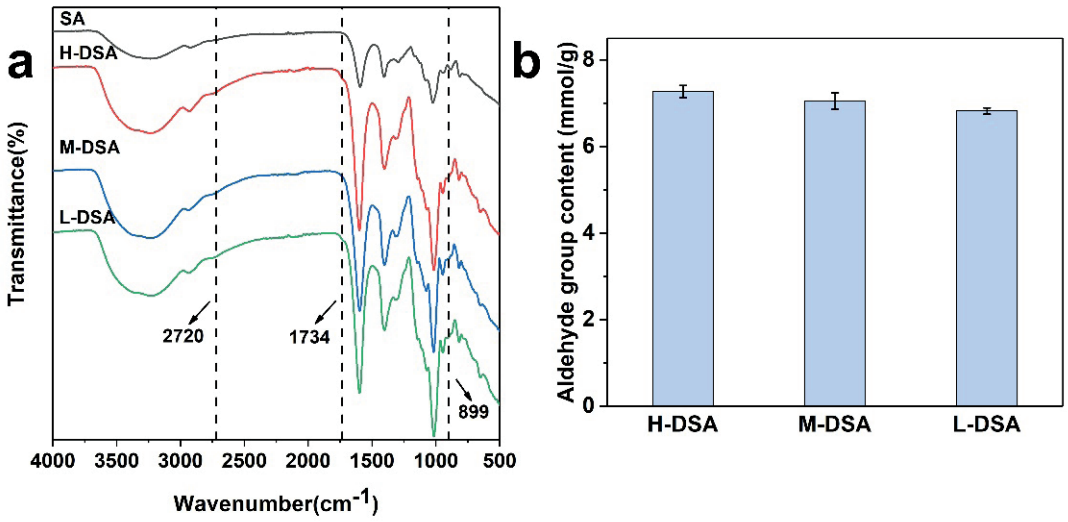

Figure 1. FT–IR spectra of SA and DSAs **(a)** and aldehyde group content of DSAs **(b)**

Observation of DTAF–DSA during tanning

Several pieces of pickled cattle hide (1.5 g each, from symmetrical parts of butt along the backbone) were rewetted and depickled to pH 7.0 with sodium bicarbonate. Then they were divided into eighteen groups (two pieces in each group) for the following tanning trials. DTAF–DSAs with different molecular weights were used as the tanning agents. Every six groups were tanned with 4% of one type of tanning agent (a mixture of DTAF–DSA and DSA with the mass ratio of 1:4) and 100% water (based on limed weight) at 25°C for 15 min, 45 min, 1 h, 2 h, 2.5 h and 4 h, respectively. After tanning, the samples were cut into vertical sections (thickness, 20 μm) using a freezing microtome (CM1950, Lecia, Germany). Sections were observed via an inverted fluorescence microscope (DMi8, Lecia, Germany) to locate DTAF–DSA in the leather. The relative content of DTAF–DSA in the leather was analyzed from the micrograph by Image J software.[39] Furthermore, the sections were stained with hematoxylin and eosin (HE). The bright field photographs of HE stained sections were obtained by an inverted fluorescence microscope (DMi8, Lecia, Germany) to show the collagen fiber structure.

Results and Discussion

Characteristics of DSA

FT–IR analysis and aldehyde group content determination were performed to verify if aldehyde groups were formed on DSA after periodate oxidation of SA. Compared with the infrared spectrum of SA, the infrared spectrum of DSAs showed new absorption peaks of aldehyde carbonyl group at 899 cm^{-1} (stretching vibration of hemiacetal), 1734 cm^{-1} (C=O stretching vibration of aldehyde group) and 2720 cm^{-1} (C–H stretching vibration of aldehyde group)[40-42] (Figure 1a). Moreover, DSAs with different molecular weights exhibited similar aldehyde group content of 6.8–7.3 mmol/g (Figure 1b). These results indicated that aldehyde groups were successfully introduced into DSA.

Characteristics of DTAF–DSA

Typical functional groups of DSA, including hydroxyl (–OH), carboxyl (–COOH), and aldehyde group (–CHO) were available for fluorescence labeling. Dichlorotriazine, the reactive group of DTAF, has strong reactivity with hydroxyl of DSA through a nucleophilic substitution reaction in alkaline conditions (pH > 9) at room temperature.[43] Thus, DSA could be labeled by DTAF (see Figure 2).

Purification is needed to remove the excessive DTAF because the unreacted fluorescein residues will interfere with the tracing of DTAF–DSA in leather. Column chromatography was conducted using a Sephadex G-25 gel-filtration column to remove the unreacted DTAF (Figure 3). The reaction mixtures were separated into different fractions, and the main component in relatively high purity was collected as DTAF–DSA.

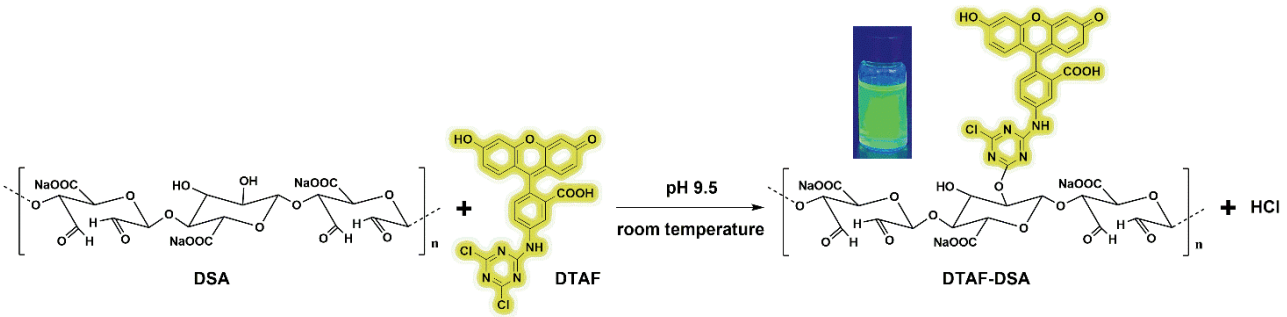

Figure 2. Schematic diagram of the DTAF labeling reaction with DSA.

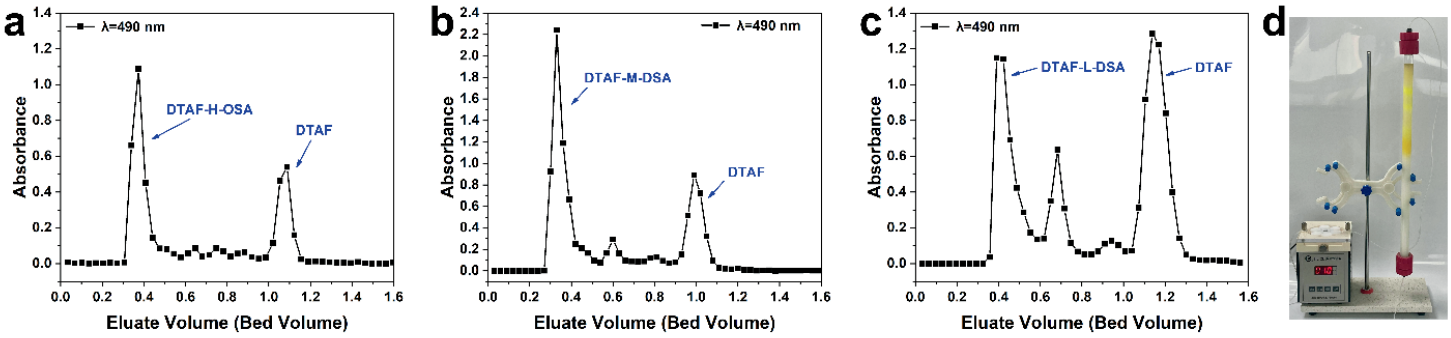

Figure 3. Chromatogram of **(a)** DTAF–H–DSA, **(b)** DTAF–M–DSA and **(c)** DTAF–L–DSA on **(d)** Sephadex G-25 gel-filtration column (1.6 cm × 50 cm). The column was eluted with borax/boric acid buffer (pH 9.0) at a rate of 0.06 mL/min.

The molecular weight of a tanning agent has a significant influence on its mass transfer and distribution in leather fiber network.[19] The molecular weights of DSA and DTAF–DSA with different sizes were determined before and after labeling. The molecular weights of the unlabeled DSAs showed a gradual decline because of the ethanol fractional precipitation (Table I). The molecular weights of DSAs decreased after labeling by DTAF. The most probable reason is DSA degradation in the alkaline labeling conditions (pH 9.5, 24 h). Another possible cause is the loss of unlabeled components in DSA during column chromatography. Even so, the DTAF labeled DSAs exhibited molecular weight gradients from approx. 25000 to 10000, which favored the investigation of the effect of DSA molecular weight on the mass transfer of the tanning agent in leather. The PDI of DSAs meant that DSAs had relatively narrow distribution. PDI of a tanning agent will influence its mass transfer in leather. In our previous work,[18] DSA with wide molecular weight distribution (high PDI) could endow leather with satisfactory comprehensive properties. Hence, an effective approach to characterize the mass transfer behavior of dialdehyde polysaccharide tanning agent could explore the effect of mass transfer on the tanning performance and help design PDAs with better tanning effect which have more suitable molecular weight and PDI.

The fluorescence spectra of DTAF, unlabeled DSA and purified DTAF–DSA were recorded at excitation wavelength of 492 nm (Figure 4). DTAF and DTAF–DSA exhibited the maximum emission at 515.2 nm, while unlabeled DSA showed absence of fluorescence. This result indicated that DTAF could successfully graft on DSA and give DSA detectable fluorescence to realize the visualization of mass transfer of DSA in leather fiber network.

The effects of pH and temperature on the fluorescent intensity of DTAF–DSA were explored to verify if the fluorescent DSA is visualized under the tanning conditions. As shown in Figures 5(a)

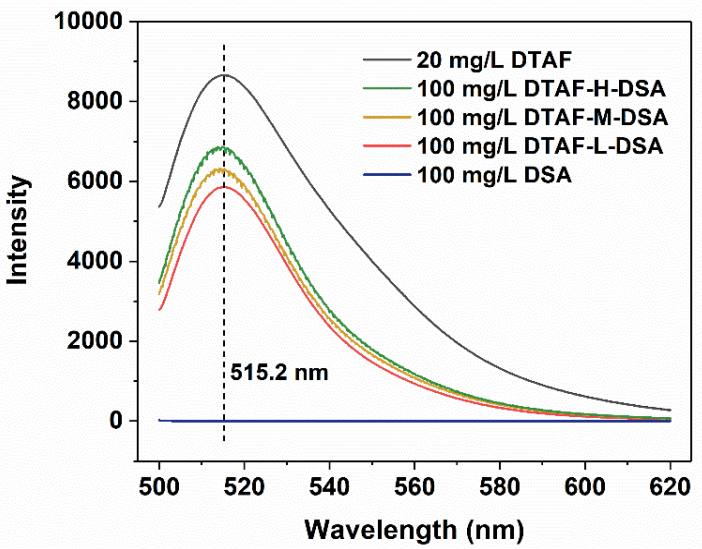

Figure 4. Fluorescence emission spectra of DTAF (20 mg/L), DTAF–H–DSA (100 mg/L), DTAF–M–DSA (100 mg/L), DTAF–L–DSA (100 mg/L) and DSA (100 mg/L) obtained using excitation wavelength of 492 nm (the excitation maximum of DTAF)

Table I

Molecular weight of DSA and DTAF–DSA

	M_w	PDI		M_w	PDI
H–DSA	77834	2.87	DTAF–H–DSA	24653	3.90
M–DSA	54972	2.50	DTAF–M–DSA	17241	3.60
L–DSA	26200	1.64	DTAF–L–DSA	9842	1.82

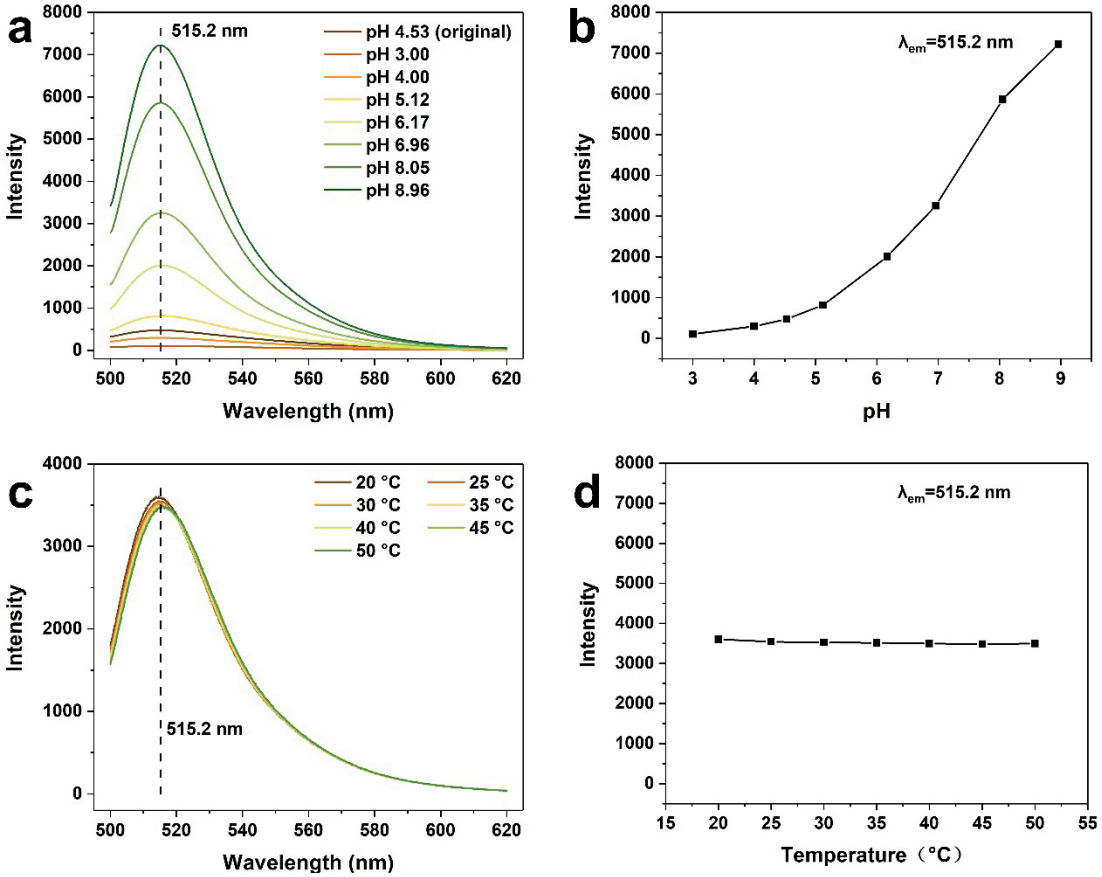

Figure 5. Fluorescence emission spectra of DTAF–L–DSA at different pH values **(a)** and temperatures **(c)**. Effects of pH **(b)** and temperature **(d)** on the fluorescent intensity of DTAF–L–DSA at emission wavelength of 515.2 nm. The excitation wavelength was 492 nm

and 5(b), the fluorescent intensity of DTAF–DSA is sensitive to pH changes. The intensity increased significantly as the pH value rose from 3 to 9. Thus, the recommended application pH value for DTAF–DSA was higher than 6.0. The isoelectric point of pickled hide is around 5.5~6.0.[44-45] When the pH is higher than 6.0, the pickled hide is negatively charged, which favors the penetration of DSA (rich in carboxyl groups, also negatively charged over pH 6.0) into leather. Considering the aldehyde tanning mechanism and previous experience of DSA tanning,[17,18] pickled hide was depickled to pH 7.0 before tanning to ensure the fluorescent tracing of DTAF–DSA during tanning. The penetration and distribution of DSA is expected to be accurately observed under this condition. As shown in Figures 5(c) and 5(d), there was little change in the fluorescence intensity of DTAF–DSA in the temperature range of 20°C to 50°C. Hence, 25°C was chosen for fluorescent tracing of DTAF–DSA as well as tanning.

Fluorescent tracing of DTAF–DSA in Leather

Pickled hide was depickled to pH 7.0 and then tanned by a mixture of DSA and DTAF–DSA at 25°C. The trace of DTAF–DSA in the leather fiber network was observed using a fluorescence microscope at different time points. The cross-sections of leather are shown in Figure 6. Collagen fibers in pickled hide were stained red with HE, and DTFA–DSA (green) were visible within collagen fiber network from the fluorescence micrographs. Image J software quantitatively analyzed the relative content of DTAF–DSA from Figure 6 and clearly showed the distribution of DSA in the leather (see Figure 7). The rewetted and depickled hides as control exhibited no detectable fluorescence because fluorescent labeled DSA was not added before tanning. Fluorescence appeared in both grain and flesh sides in the initial period of tanning, while no fluorescence was observed in the middle layer of hide. This result indicated that DSA started to permeate from the grain and flesh layers. The fluorescence brightness of the middle layer gradually increased with tanning time, which illuminated that DSA transferred to the core of the hide from grain and flesh. After a period of tanning, the fluorescence brightness along the cross-section was uniform and reached a plateau as shown in Figure 7. The phenomenon suggested that DSA fully penetrated in collagen fiber network.

DSAs with varying molecular weights were applied in tanning and exhibited different mass transfer characteristics. DTAF–H–DSA (M_w 24653) fully penetrated and evenly distributed in the cross-section of leather after 120 min. The penetration durations for DHAF–M–DSA (M_w 17241) and DTAF–L–DSA (M_w 9842) were shortened to 105 min and 60 min, respectively. These results suggested that the molecular weight of DSA tanning agent played a critical role in the penetration rate of DSA. The penetration rate increased with decreasing molecular weight of DSA. This regularity

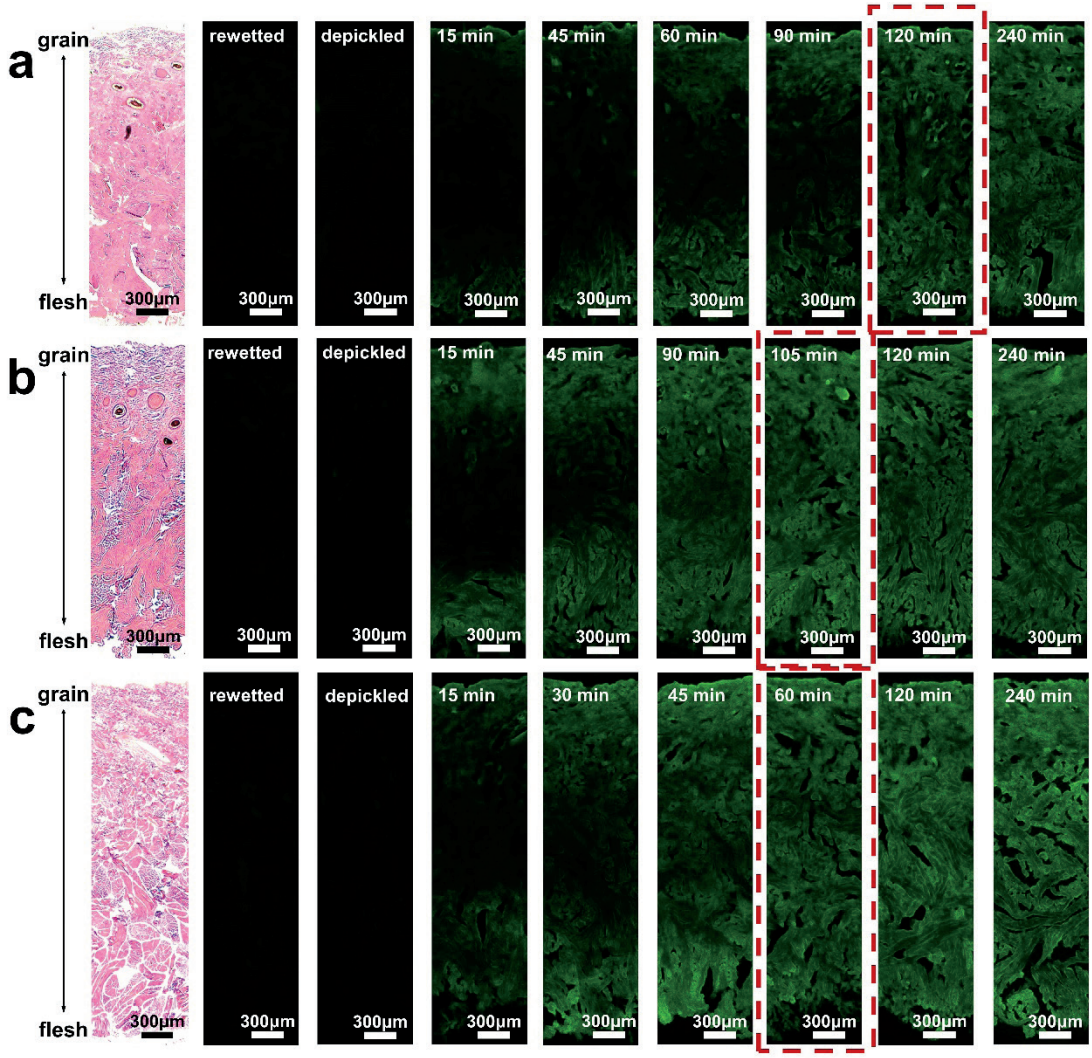

Figure 6. HE–stained bright field micrographs and fluorescence micrographs of cross-sections of leather tanned with a mixture of DSA and DTAF–DSA. **(a)** H–DSA and DTAF–H–DSA were used. **(b)** M–DSA and DTAF–M–DSA were used. **(C)** L–DSA and DTAF–L–DSA were used

is in accordance with previous results regarding the penetration of enzymes[23,46] and acrylic resins.[26]

The results above demonstrated that the penetration behavior of fluorescent labeled dialdehyde polysaccharide tanning agent in leather matrix could be preliminarily visualized and semiquantified by using fluorescent tracing technique. In future research, high-resolution fluorescence microscopic techniques can be used to further observe the distribution of fluorescent labeled tanning agents within the hierarchical microstructure of leather. Thus, the issue of the multi-scale mass transfer and crosslinking of tanning agents in leather could be explored from a fresh perspective, and the tanning mechanism is expected to be deeply revealed.

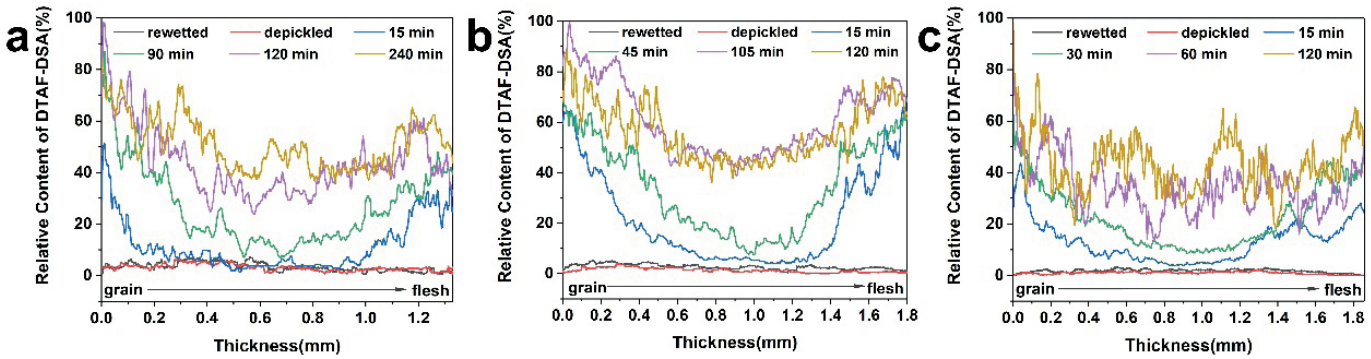

Figure 7. Distribution of **(a)** DTAF–H–DSA, **(b)** DTAF–M–DSA and **(c)** DTAF–L–DSA in the tanned leather. The relative contents of DTAF–DSA was quantified by analysis of the fluorescence micrographs in Figure 5 using Image J software

Conclusions

DSA tanning agent can be successfully labeled by fluorescein DTAF through covalent binding between hydroxyl of DSA and dichlorotriazine of DTAF. This provides a convenient fluorescent labeling method for polysaccharide-based tanning agents. Furthermore, the penetration and location of fluorescent labeled DSA tanning agent in leather can be visualized and preliminarily investigated by the fluorescent tracing technique. This provides an effective means to probe the mass transfer characteristics and help evaluate tanning effects of polysaccharide-based tanning agents. The results will help reveal the tanning mechanism and develop novel tanning agents.

Acknowledgement

This work was financially supported by the National Natural Science Foundation of China (22278280), Sichuan Science and Technology Program (2022JDRC0029), and the Tianfu Ten-thousand Talents Program of Sichuan Province.

References

1. Yu Y., Wang H., Wang Y. N., Zhou J. F., Shi B.; Construction of a Chrome-free Tanning System Based on Highly-oxidized Starch–Zirconium Complexes. *JALCA* **117**, 87-95, 2022.
2. Inbasekar C., Rao J. R., Fathima N.N.; Strategizing the Development of a Metal- and Formaldehyde-Free Tanning Process Using (3,5-Dimethyl-1H,3H,5H-oxazolo[3,4-c]oxazol-7a(7H)-yl) Methanol Heterocyclic Derivative Oxazolidine and Polyallylamine. *ACS Sustain. Chem. Eng.* **9**, 15053-15062, 2021.
3. Shen Y. M., Ma J. Z., Fan Q. Q., Gao D. G., Yao H.; Strategical development of chrome-free tanning agent by integrating layered double hydroxide with starch derivatives. *Carbohydr. Polym.* **304**, 120511, 2023.
4. Hedberg Y. S.; Chromium and leather: a review on the chemistry of relevance for allergic contact dermatitis to chromium. *J. Leather Sci. Eng.* **2**, 20, 2020.
5. Xu T., Jiang X. F., Tang Y. L., Zeng Y. H., Zhang W. H., Shi B.; Oxidation of trivalent chromium induced by unsaturated oils: a pathway for hexavalent chromium formation in soil. *J. Hazard. Mater.* **405**, 124699, 2021.
6. Xu T., Nan F., Jiang X. F., Tang T. L., Zeng Y. H., Zhang W. H., Shi B.; Effect of soil pH on the transport, fractionation, and oxidation of chromium (III). *Ecotox. Environ. Safe.* **195**, 110459, 2020.
7. Yu Y., Lin Y. R., Zeng Y. H., Wang Y. N., Zhang W. H., Zhou J. F., Shi B.; Life cycle assessment for chrome tanning, chrome-free metal tanning, and metal-free tanning systems. *ACS Sustain. Chem. Eng.* **9**, 6720-6731, 2021.
8. Guo X. R., Yu Y., Wang Y. N., Shi B.; Oxidized maltodextrin: a novel ligand for aluminum–zirconium complex tanning. *JALCA* **116**, 155-161, 2021.
9. Jiang Z. C., Ding W., Fan J. J., Liao Y. H., Remón J., Shi B.; Biomass derived oligosaccharides for potential leather tanning. *J. Leather Sci. Eng.* **5**, 7, 2023.
10. Chen H., Hu Y., Li S. Q., Chen L. W., Yi J., Shan Z. H., Dai R.; The tanning performance of dialdehyde cellulose prepared by electrochemical oxidation system. *J. Soc. Leather Thchnol. Chem.* **103**, 305-311, 2019.
11. Ding W., Yi Y. D., Wang Y. N., Zhou J. F., Shi B.; Peroxide-periodate co-modification of carboxymethylcellulose to prepare polysaccharide-based tanning agent with high solid content. *Carbohydr. Polym.* **224**, 115169, 2019.
12. Yi Y. D., Zhang Y., Mansel B., Wang Y. N., Prabakar S., Shi B.; Effect of dialdehyde carboxymethyl cellulose cross-linking on the porous structure of the collagen matrix. *Biomacromolecule* **23**, 1723-1732, 2022
13. Ozkan C. K., Ozgunay H., Akat H.; Possible use of corn starch as tanning agent in leather industry: Controlled (gradual) degradation by H2O2. *Int. J. Biol. Macromol.* **122**, 610-618, 2019..
14. Hao D. Y., Wang X. C., Liu X. H., Su R. R., Duan Z. J., Dang X. G.; Chrome-free tanning agent based on epoxy-modified dialdehyde starch towards sustainable leather making. *Green Chem.* **23**, 9693-9703, 2021.
15. Yu Y., Wang Y. N., Ding W., Zhou J. F., Shi B.; Preparation of highly-oxidized starch using hydrogen peroxide and its application as a novel ligand for zirconium tanning of leather. *Carbohydr. Polym.* **174**, 823-829, 2017.
16. Yu Y., Wang H., Wang Y. N., Zhou J. F., Shi B.; Chrome-free synergistic tanning system based on biomass-derived hydroxycarboxylic acid–zirconium complexes. *J. Clean Prod.* **336**, 130428, 2022.
17. Ding W., Zhou J. F., Zeng Y. H., Wang Y. N., Shi B.; Preparation of oxidized sodium alginate with different molecular weights and its application for crosslinking collagen fiber. *Carbohydr. Polym.* **157**, 1650-1656, 2017.
18. Ding W., Yi Y. D., Wang Y. N., Zhou J. F., Shi B.; Preparation of a highly effective organic tanning agent with wide molecular weight distribution from bio-renewable sodium alginate. *Chemistryselect* **3**, 12330-12335, 2018.
19. Ding W., Wang Y. N., Zhou J. F., Shi B.; Effect of structure features of polysaccharides on properties of dialdehyde polysaccharide tanning agent. *Carbohydr. Polym.* **201**, 549-556, 2018.
20. Nypelö T., Berke B., Spirk S., Sirvio J. A.; Review: Periodate oxidation of wood polysaccharides—Modulation of hierarchies. *Carbohydr. Polym.* **252**, 117105, 2021.
21. Yu Y., Zeng Y. H., Wang Y. N., Liang T., Zhou J. F., Shi B.; Inverse chrome tanning technology: a practical approach to minimizing Cr (III) discharge. *JALCA* **115**, 176-182, 2020.
22. Zeng Y. H., Yang Q., Wang Y. N., Zhou J. F., Shi B.; Neutral Protease Assisted Low-sulfide Hair-save Unhairing Based on pH-sensitivity of Enzyme. *JALCA* **111**, 345-353, 2016.
23. Song Y., Wu S. Q., Yang Q., Liu H., Zeng Y. H., Shi B.; Factors affecting mass transfer of protease in pelt during enzymatic bating process. *J. Leather Sci. Eng.* **1**, 4. 2019.

24. Wang H., Lei C., Zeng Y. H., Song Y., Zhang Q. X., Shi B.; Reversible inhibition of trypsin activity with soybean flour in hide bating process for leather quality improvement. *Ind. Crop. Prod.* **161,** 113222, 2021.
25. Zeng Y. H., Song Y., Li J., Zhang W. H., Shi B.; Visualization and Quantification of Penetration/Mass Transfer of Acrylic Resin Retanning Agent in Leather using Florescent Tracing Technique. *JALCA* **111**, 398-405, 2016.
26. Song Y., Zeng Y. H., Xiao K. L., Wu H. P., Shi B.; Effect of molecular weight of acrylic resin retanning agent on properties of leather. *JALCA* **112**, 128-134, 2017.
27. Song Y., Zeng Y. H., Shi B.; Effect of histological feature of leather on acrylic resin retanning. *J. Soc. Leather Technol. Chem.* **102**, 149-154, 2018.
28. Song Y., Wang Y. N., Zeng Y., Wu H. P., Shi B.; Quantitative determinations of isoelectric point of retanned leather and distribution of retanning agent. *JALCA* **113**, 232-238, 2018.
29. Huang W. L., Song Y., Yu Y., Wang Y. N., Shi B.; Interaction between retanning agents and wet white tanned by a novel bimetal complex tanning agent. *J. Leather Sci. Eng.* **2**, 8, 2020.
30. Du J. X., Shi L., Peng B. Y.; Real-time monitoring of the penetration of amphiphilic acrylate copolymer in leather using a fluorescent copolymer as tracer. *Microsc. Res. Tech.* **78**, 1146-1153, 2015.
31. Du J. X., Shi L., Peng B. Y.; Amphiphilic acrylate copolymer fatliquor for ecological leather: Influence of molecular weight on performances. *J. Appl. Polym. Sci.* **133**, 43440, 2016.
32. Wen H. M., Wang Y. L., Zhu H. X., Jin L. Q., Zhang F. F.; A Fluorescent Tracer Based on Castor Oil for Monitoring the Mass Transfer of Fatliquoring Agent in Leather. *Materials* **15**, 1167, 2022.
33. Song Y., Wu S. Q., Wang Y. N. Zhu M., Yi Y. D., Zeng Y. H., Shi B.; Visualization of penetration and reaction of aldehyde tanning agent in leather using fluorescence technique. *JALCA* **115**, 248-254, 2020.
34. Ding W., Wang Y. N., Zhou J. F., Liu H. T., Pang X. Y., Shi B.; Investigations on the general properties of biomass-based aldehyde tanned sheep fur for its selective post-tanning processing. *J. Leather Sci. Eng.* **3**, 5, 2021.
35. Liu, B. H., Wei, Z., Wang, Y. N., Shi, B.; Preparation of oxidized poly (2-hydroxyethyl acrylate) with multiple aldehyde groups by TEMPO-mediated oxidation for gelatin crosslinking. *JALCA,* **114,** 163-170, 2019.
36. Abitbol, T., Palermo, A., Moran-Mirabal, J. M.; Fluorescent labeling and characterization of cellulose nanocrystals with varying charge contents. *Biomacromolecules.* **14,** 3278–3284, 2013.
37. Li, Q. J., Yi, Y. D., Wang, Y. N., Li, J., Shi, B. Effect of cationic monomer structure on the aggregation behavior of amphoteric acrylic polymer around isoelectric point. *J. Leather Sci. Eng*, **4**, 4, 2022.
38. Fu, X., Dai, J. H., Guo, X. W., et al. Suppression of oligomer formation in glucose dehydration by CO_2 and tetrahydrofuran. *Green Chem.* **19,** 3334–3343, 2017.
39. Gupta, G. P., Nguyen, D. X., Chiang, A. C., Bos, P. D., Kim, J. Y., Nadal, C., Gomis, R. R., Manova-Todorova, K., Massague, J.; Mediators of vascular remodelling co-opted for sequential steps in lung metastasis. *Nature.* **446,** 765-770, 2007.
40. Wang, P., He, H. W., Cai, R., Tao, G., Yang, M. R., Zuo, H., Umar, A., Wang, Y. J.; Cross-linking of dialdehyde carboxymethyl cellulose with silk sericin to reinforce sericin film for potential biomedical application. *Carbohydr. Polym.* **212,** 403-411, 2019.
41. Khadiran, T., Hussein, M. Z., Zainal, Z., Rusli, R.; Shape-stabilised n-octadecane/activated carbon nanocomposite phase change material for thermal energy storage. *J. Taiwan Inst. Chem. Eng.* **55,** 189-197, 2015.
42. Wan, Y. C., Chen, Y., Cui, Z. X., Ding, H., Gao, S. F., Han, Z., Gao, J. K.; A promising form-stable phase change material prepared using cost effective pinecone biochar as the matrix of palmitic acid for thermal energy storage. *Sci Rep.* **9,** 11535, 2019.
43. De Hoog, P., Gamez. P., Driessen, W. L., Reedijk, J.; New polydentate and polynucleating N-donor ligands from amines and 2,4,6-trichloro-1,3,5-triazine. *Tetrahedron Lett.* **43,** 6783–6783, 2002.
44. Wang, Y. N., Huang, W. L., Zhang, H. S., Tian, L., Zhou, J. F., Shi, B.; Surface charge and isoelectric point of leather: A novel determination method and its application in leather making. *JALCA,* **112,** 224-231, 2017.
45. Wang, Y. N., Hu, L. Y.; Essential role of isoelectric point of skin/leather in leather processing. *J. Leather Sci. Eng*, **4,** 25, 2022.
46. Liu, C., Chen, X. Y., Zeng, Y. H., Shi, B.; Effect of the surface charge of the acid protease on leather bating performance. *Process Biochem.* **121,** 330-338, 2022.